Available online at www.sciencedirect.com
ScienceDirect
Journal of Power Sources 178 (2008) 439–444
JOURNAL OF POWER SOURCES
www.elsevier.com/locate/jpowsour

Short communication

Synthesis of $LiNi_{1/3}Co_{1/3}Mn_{1/3}O_2$ as a cathode material for lithium battery by the rheological phase method

Haibo Ren, Yourong Wang, Daocong Li, Lihua Ren, Zhenghe Peng *, Yunhong Zhou

Department of Chemistry, Wuhan University, Wuhan 430072, PR China

Received 30 July 2007; received in revised form 3 December 2007; accepted 5 December 2007
Available online 14 December 2007

Abstract

$LiNi_{1/3}Co_{1/3}Mn_{1/3}O_2$ is prepared by a rheological phase method. Homogeneous precursor derived from this method is calcined at 800 °C for 20 h in air, which results in the impressive differences in the morphology properties and electrochemical behaviors of $LiNi_{1/3}Co_{1/3}Mn_{1/3}O_2$ in contrast to that obtained by a solid-state method. The microscopic structural features of $LiNi_{1/3}Co_{1/3}Mn_{1/3}O_2$ are investigated using scanning electron microscopy (SEM), X-ray diffraction (XRD). The electrochemical properties of $LiNi_{1/3}Co_{1/3}Mn_{1/3}O_2$ are carried out by charge–discharge cycling test. All experiments show that the microscopic structural features and the morphology properties are deeply related with the electrochemical performances. The obtained results suggest that the rheological phase method may become an effective route to prepare $LiNi_{1/3}Co_{1/3}Mn_{1/3}O_2$ cathode materials for lithium battery.

Keywords: Lithium battery; Cathode material; $LiNi_{1/3}Co_{1/3}Mn_{1/3}O_2$; Electrochemical behavior; Rheological phase method

1. Introduction

In the recent years, the layered transition metal oxide $LiNi_{1/3}Co_{1/3}Mn_{1/3}O_2$ has been extensively studied since it was firstly synthesized by Ohzuku and Makimura [1] in 2001. As a promising cathode material for lithium ion batteries, it has a high discharge capacity, high rate capability and good cycling performance. These advantages of $LiNi_{1/3}Co_{1/3}Mn_{1/3}O_2$ are attributed to its typical hexagonal α-$NaFeO_2$ structure with a space group of $R\bar{3}m$. In this structure, Li ions, the transition metal (Ni, Co, Mn) ions and O ions take 3a, 3b and 6c sites, respectively. The predominant oxidation states of Ni, Co, Mn ions are +2, +3, +4, which have been indicated by XPS studies [2,3] and calculation [4–6] on the structure. Ni and Co act as the electrochemically active species during cycling in the voltage range of >2.5 V, while Mn^{4+} is electrochemically inert not to participate in the redox reaction and functions as stable framework, so that the stabilization of the structure is achieved leading to the well-cycling performance [2].

Unfortunately, due to the complicated composition, the cathode properties of $LiNi_{1/3}Co_{1/3}Mn_{1/3}O_2$ should be sensitively dependent on microscopic features like the distribution of transition metal and the particle morphology. As a result, it is difficult to prepare this complicated material, and the rate capability of this material depends on the synthetic route which has greater influence on the particle morphology. Therefore, it is important for $LiNi_{1/3}Co_{1/3}Mn_{1/3}O_2$ to select suitable preparation method. To synthesize this material, many researchers employed different methods, such as mixed hydroxide method [7], sol–gel method [5], solid-state method [8] and molten salt method [9], and some better results have been achieved.

In this paper, we introduced a novel method, the rheological phase method [10] to synthesize $LiNi_{1/3}Co_{1/3}Mn_{1/3}O_2$. The rheological phase method is the process of preparing compounds or materials from a solid–liquid rheological mixture. The solid reactants are fully mixed in a proper molar ratio, and made up by a proper amount of water or other solvents to a container in which the solid powders and liquid substances are uniformly distributed, so the surface area of the solid particles can be utilized

* Corresponding author. Tel.: +86 27 87218254; fax: +86 27 68754067.
E-mail address: pengzh@chem.whu.edu.cn (Z. Peng).

0378-7753/$ – see front matter © 2008 Elsevier B.V. All rights reserved.
doi:10.1016/j.jpowsour.2007.12.004

more efficiently than that in the solid-state phase. Because the solid and liquid sections are in contact with each other, it is convenient for the heat exchange and should facilitate the diffusion of ions dissolved in solvent into the solid particles [11]. After further reaction, the final product or precursor can be obtained. By this method, many functional materials and compounds with novel structures and properties have been obtained [10,12].

2. Experimental

2.1. Synthesis of $LiNi_{1/3}Co_{1/3}Mn_{1/3}O_2$

A rheological phase method was employed to synthesize $LiNi_{1/3}Co_{1/3}Mn_{1/3}O_2$. $LiOH{\cdot}H_2O$, $Ni(OH)_2$, Co_2O_3, MnO_2 were used as the starting materials in quantities corresponding to 0.1 mol stoichiometric $LiNi_{1/3}Co_{1/3}Mn_{1/3}O_2$ with 6% excess of Li. These reagents were mixed, thoroughly ground and then transferred into a cylindrical Teflon-lined container. A proper amount of distilled water was added into the container to become a rheological body. The container was sealed in a stainless autoclave at 90 °C for 6 h. After reaction, the rheological body was dried at 120 °C for 6 h and ground again to obtain a homogeneous precursor. The precursor was calcined at 800 °C for 20 h in air to yield $LiNi_{1/3}Co_{1/3}Mn_{1/3}O_2$ (denoted as RP).

As a contrast to the rheological phase method, $LiNi_{1/3}Co_{1/3}Mn_{1/3}O_2$ was also carried out by a solid-state method in this work (denoted as SP). The starting materials, proportion and calcined conditions were the same as those of the rheological phase method.

2.2. Measurements

X-ray diffraction measurements of the $LiNi_{1/3}Co_{1/3}Mn_{1/3}O_2$ materials were carried out using X-ray diffraction (Shimadzu XRD-6000) with Cu Kα radiation (λ = 1.54056 Å). Lattice parameters and unit-cell volumes were calculated by a least

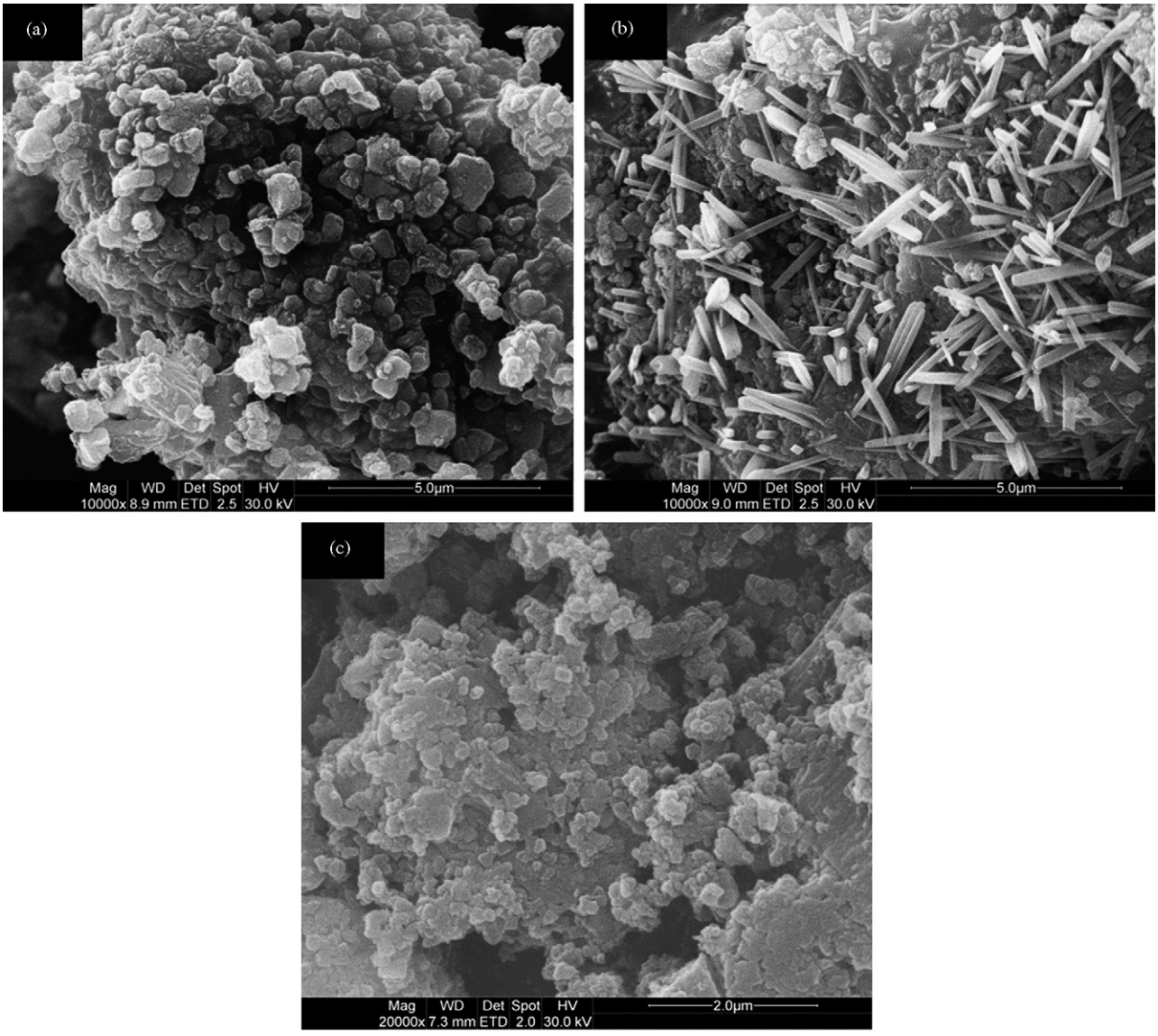

Fig. 1. SEM micrographs of: (a) SP, (b) RP and (c) RP precursor after drying.

squares method with FullProf Suite program. Particle morphology of the powders after calcinations was observed using a scanning electron microscope (SEM, QUANTA-200). The specific areas of $LiNi_{1/3}Co_{1/3}Mn_{1/3}O_2$ samples were deduced from nitrogen adsorption experiments (BET method).

Electrochemical charge–discharge experiments were performed by assembling model test cells. Test cathode electrodes were prepared by mix 80:15:5 (mass ratio) of active material, acetylene black and PTFE binder, respectively, in isopropyl alcohol. The model test cells were assembled with the electrode prepared above as cathode, lithium metal as anode, and Celgard 2300 film as separator in an argon-filled glove box. The electrolyte was 1 M $LiClO_4$ dissolved in EC+DMC (1:1 volume ratio). All tests were performed at room temperature.

3. Results and discussion

3.1. Morphology of the particles

SEM micrographs of the two samples of $LiNi_{1/3}Co_{1/3}Mn_{1/3}O_2$ (SP and RP) and the RP precursor after drying are illustrated in Fig. 1. SP powder consists of grains of average 1 μm with no characteristic morphology and most particles are badly aggregated. As we know, Agglomerations leads to the decrease of specific surface area of particles, which means that the electrochemical capability might descend [13]. The morphology of RP, however, is obviously different from that of SP. RP powder is composed of grains and rods with an average diameter of about 0.3 μm and a length of about 3 μm. Although some particles are also aggregated, the phenomenon aggregated is availably decreased due to existing rod-like shape particles and its specific surface area, 1.6628 $m^2\,g^{-1}$, is bigger than that of SP, 1.2146 $m^2\,g^{-1}$. As is well known, the influence of particle size, morphology and surface area to the battery performance is of great importance. We believe that differences of RP and SP in size, morphology and surface area should result in differences in their electrochemical performance.

In addition, the rod-like shape particles are not found in the RP precursor from Fig. 1c, which indicates that the rod-like shape particles in the RP sample only forms in the process of calcination. However, though there are no appearances of rods in the RP precursor, the rheological phase process preparing the RP precursor plays a vital role in the development of the rods in the calcination step.

3.2. Structure analysis

Fig. 2 shows typical XRD patterns of the synthesized $LiNi_{1/3}Co_{1/3}Mn_{1/3}O_2$ materials in two different methods. All peaks are sharp and well-defined, suggesting that compounds are generally well crystallized, which can be indexed to the hexagonal α-$NaFeO_2$ structure (space group: $R\bar{3}m$) without any impurity peaks. The peak splits of (0 0 6)/(1 0 2) and (1 0 8)/(1 1 0) doublets, being especially obvious for the RP material, indicate the formation of a highly ordered layer structure [3,14]. The lattice parameters of the synthesized materials were calculated by least square method using 10-diffraction

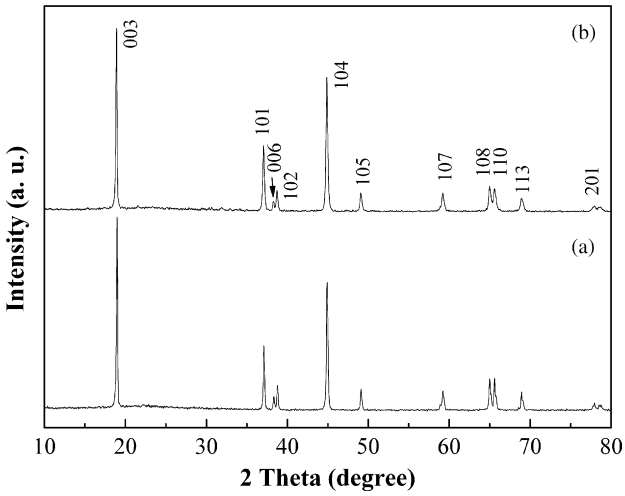

Fig. 2. XRD patterns of $LiNi_{1/3}Co_{1/3}Mn_{1/3}O_2$ prepared from the rheological phase method (a), the solid-state method (b).

Table 1
Lattice parameters of $LiNi_{1/3}Co_{1/3}Mn_{1/3}O_2$ prepared by different methods

Samples	a (Å)	c (Å)	c/a	$I_{(003)}/I_{(104)}$
RP	2.8433	14.1887	4.99	1.56
SP	2.8471	14.1785	4.98	1.38
Literature [9]	2.8467	14.1967	4.99	1.6
Literature [13]	2.8496	14.2045	4.98	1.86
Literature [1]	2.867	14.246	4.969	–
Literature [2]	2.864	14.233	4.969	–

lines and tabulated in Table 1. As is shown, the sample RP has smaller lattice parameters, a and c compared to those reported [1,2] while a larger triangle distortion, c/a, but it is similar to some results of Reddy et al. [9,13]. These differences in lattice parameters are likely to coming from different preparation conditions and methods. Moreover, Reddy et al. [9] considered these smaller lattice parameters might be due to smaller cation mixing and better ordering of the transition metal ions in the metal-layer. Lattice parameters are closely related with atomic distribution (e.g. cation mixing) in hexagonal oxide cathode material. A partial interchange of occupancy of Li ions and transition metal ions will give rise to cation mixing in the structure, which can deteriorate battery performances [15]. Hwang et al. [16] believed that the intensity ratio of the (0 0 3) and (1 0 4) peaks ($I_{(003)}/I_{(104)}$) could be used to identify the cation mixing degree. Generally, when the value of intensity ratio is more than 1.2, the cation mixing is small with good layered structure. In the present study, the $I_{(003)}/I_{(104)}$ ratios of RP and SP are 1.56 and 1.38, respectively, indicating no undesirable cation mixing takes place. Especially, RP holds more excellent structural integrity (bigger $I_{(003)}/I_{(104)}$), i.e. lower cation mixing. Therefore, it can be expected that the sample RP can display better electrochemical performance than the sample SP can.

3.3. Electrochemical characteristics

The electrochemical charge–discharge experiments for the two $LiNi_{1/3}Co_{1/3}Mn_{1/3}O_2$ samples were firstly carried out in

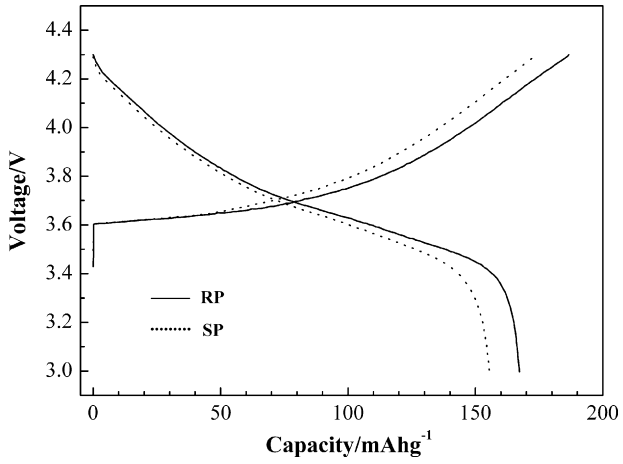

Fig. 3. Initial charge–discharge curves for $LiNi_{1/3}Co_{1/3}Mn_{1/3}O_2$ operated in the voltages range of 3–4.3 V under a current density 20 mA g^{-1}.

the voltage range 3.0–4.3 V. The constant current densities of 20, 40 and 80 mA g^{-1} were applied to working electrode. The initial charge–discharge curves at 20 mA g^{-1} are presented in Fig. 3, and the cycling performances of the two samples at different current densities are offered in Fig. 4. As shown in Fig. 3, RP and SP display smooth charge–discharge curves without any

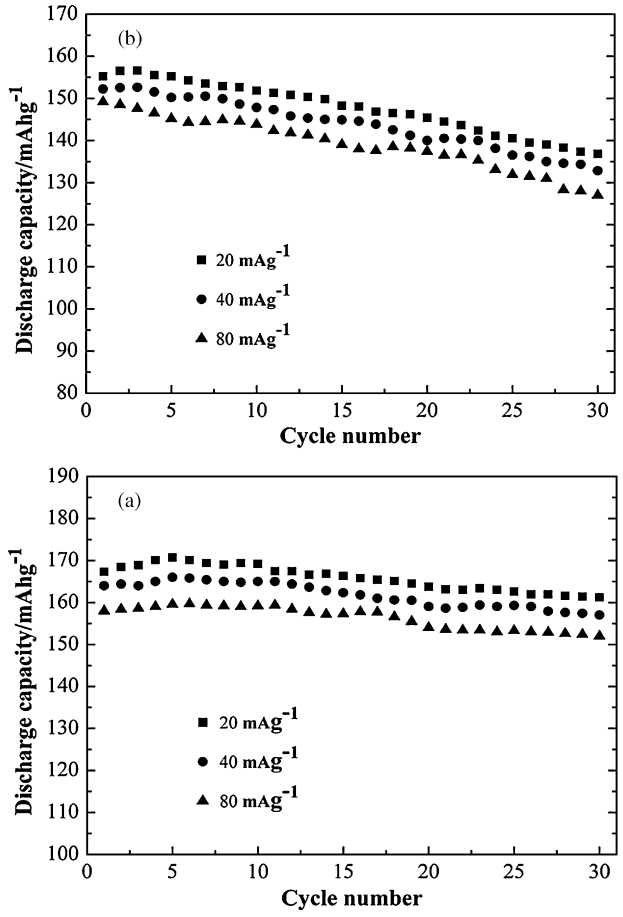

Fig. 4. Specific discharge capacity as a function of cycle number for $LiNi_{1/3}Co_{1/3}Mn_{1/3}O_2$ operated in the voltage range of 3–4.3 V at the different current densities. (a) RP, (b) SP.

plateaus, which indicate that no spinel-related phases are formed during charging and discharging. We also find that the charge and discharge curves of the sample SP are above the charge curves and below the discharge curves of the sample RP, respectively. This indicates that the electrode composed of the sample SP shows a higher polarization than that of the sample RP during the charge–discharge. The higher polarization of the sample SP compared to the sample RP may be due to the increase in cell resistant with respect to specific surface area because the sample SP has smaller specific surface area, which leads to the worse electrochemical performance of the sample SP than that of the sample RP due to low electronic conductivity [17]. At the beginning of the charging process, the voltage suddenly increases to about 3.6 V and holds at 3.6–3.8 V until the charge capacity reaches about 100 mAh g^{-1}, then gradually rises to 4.3 V. It has been well known that Ni^{2+}/Ni^{4+} coupling is electrochemical redox process in the 3.6–3.8 V for $LiNi_{1/3}Co_{1/3}Mn_{1/3}O_2$ systems. Though the initial charge–discharge curves for two samples at 40 and 80 mA g^{-1} are not displayed here, they hold similar characters with those at 20 mA g^{-1} above.

According to Figs. 3 and 4, the sample RP achieves higher discharge capacity with a slight capacity fade than that of the sample SP at same current densities. Especially, for samples RP and SP at a current density of 20 mA g^{-1}, the initial discharge capacities are 167 and 155 mAh g^{-1} with an irreversible capacity loss of about 19 and 22 mAh g^{-1}, respectively. The irreversible capacity loss might be attributed to the formation of a solid electrolyte interface (SEI) on the surface of the electrode and insufficient soaking of the electrode material during the first cycle [18]. At the end of the 30th cycle, the retained discharge capacities are 161 and 137 mAh g^{-1}, respectively, which are 96% and 88% of initial discharge capacity. It is clear that the obtained initial discharge capacity and cyclability of the sample RP are superior to those of the sample SP and are comparable to these reported [19,20].

In order to further monitor the electrochemical performance of the sample RP and SP in broader voltage and higher current density, the voltage range 2.5–4.6 V with a current density of 200 mA g^{-1} was adopted. Here, 4.6 V is chosen as the upper limit because the critical upper limit of $LiNiO_2$ and $LiCoO_2$ is 4.6 V [1,21]. As we know, when an electrode is working under bigger currents, a lot of Li^+ should be intercalated or deintercalated from electrode material at a higher speed, which demands the electrode material to have enough Li^+ used and hold better layer structure to ease the movement of Li^+. If an electrode is employed under higher voltages, the higher capacity can be gained, but the decomposition of the electrolyte at the surface of electrode material will get more serious, which brings the rapid decay of the cell capacity along with charge–discharge cycles. Therefore, it would be a severe test for the structure and performance of electrode materials if the electrodes are engaged in rigorous conditions of bigger currents and higher voltages. Fig. 5 shows the cycling performance of the sample RP and SP under given conditions. Table 2 also gives charge–discharge capacities and capacity retention rations of the two samples under the same conditions. Obviously, even though the RP material is working under rigorous conditions, the initial discharge capacity

Table 2
The charge–discharge data for RP and SP in the voltage range of 2.5–4.6 V under a current density 200 mA g^{-1}

Samples	1st cycle Q_{charge} (mAh g^{-1})	1st cycle $Q_{discharge}$ (mAh g^{-1})	30th cycle $Q_{discharge}$ (mAh g^{-1})	Capacity retention (%)
RP	227	196	186	95
SP	219	187	156	83

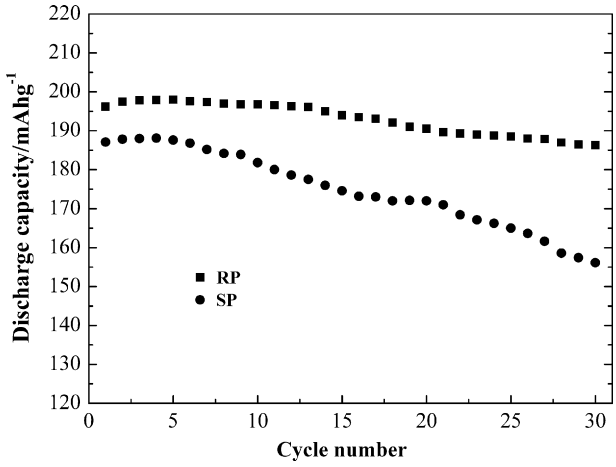

Fig. 5. Specific discharge capacity as a function of cycle number for $LiNi_{1/3}Co_{1/3}Mn_{1/3}O_2$ operated in the voltage range of 2.5–4.6 V under a current density 200 mA g^{-1}.

of 196 mAh g^{-1} can be achieved, which is almost similar to the results of the literatures [13,22], and still presents better cycling performance, retaining the discharge capacities 186 mAh g^{-1} at the end of the 30th cycle. By comparison, the SP material displays worse electrochemical performances. The initial discharge capacity is 187 mAh g^{-1} and just retains 156 mAh g^{-1} at the end of the 30th cycle. So the RP material holds more excellent structure and has lower reaction activity with the electrolyte.

Fig. 6 shows the charge–discharge curves of the two samples at the 1st and the 30th cycles, respectively. The charge–discharge curves of the RP cell at the 30th cycle are similar to those of the 1st cycle and can keep ideal charge–discharge shape, which indicates that the structure of the RP material has no obvious change and still exhibits better charge–discharge character even if it works at rigorous conditions for many cycles. However, the charge–discharge curves of the SP cell at the 30th cycle are distinctly different from those of its first cycle. Especially, its charge–discharge curves rapidly ascends and declines along with charge–discharge process, which reveals that the bigger structural changes have occurred and have unsatisfactory charge–discharge behaviors. To prove up the origin of the phenomena above, Fig. 7 gives the XRD pattern of the two electrode materials after charge–discharge 30 cycles with the voltage range 2.5–4.6 V and a current density of 200 mA g^{-1}. The RP material keeps the typical hexagonal α-$NaFeO_2$ structure well. The relative intensity of every peak remains basically unchanged and the peak splits of (0 0 6)/(1 0 2) and (1 0 8)/(1 1 0) doublets are still clearly visible, which proves that the phenomenon of cation mixing is not obvious and the layer structure exists better. When investigating carefully Fig. 7b, we can find that the XRD changes of the SP material compared with the past (Fig. 2b) are

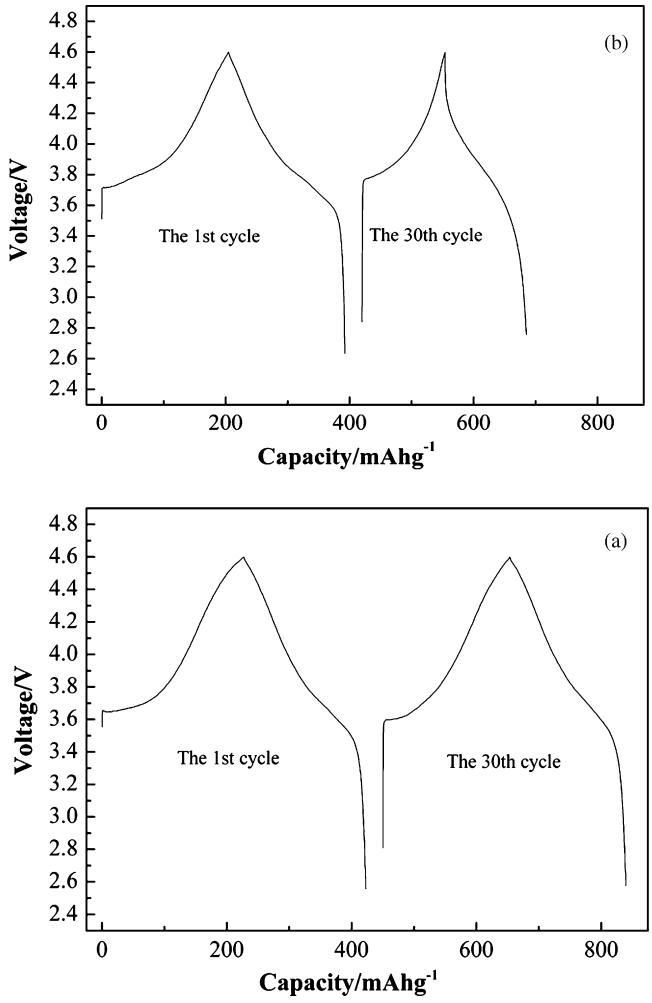

Fig. 6. The charge–discharge curves for $LiNi_{1/3}Co_{1/3}Mn_{1/3}O_2$ at the 1st and the 30th cycle. (a) RP and (b) SP.

more obvious. Not only has the relative intensity of the peaks been changed but also the peaks have slightly become broad, and the splits of the peak couples (0 0 6)/(1 0 2) and (1 0 8)/(1 1 0) have become unclear, which indicates that the phenomenon of cation mixing has seriously appeared [16] and partial crystal has also suffered destruction. These are the essential reasons why the RP cell holds better electrochemical performance after many cycles, while the electrochemical performance of the SP cell is deteriorated.

As discussed above, we know that whether in mild conditions or in poor ones, the RP material can display better electrochemical characters than the SP material can. The RP cell takes higher capacity and reveals more excellent cycling performance, which should be finally ascribed to the sample RP holding the special morphology character and the highly ordered layered structure

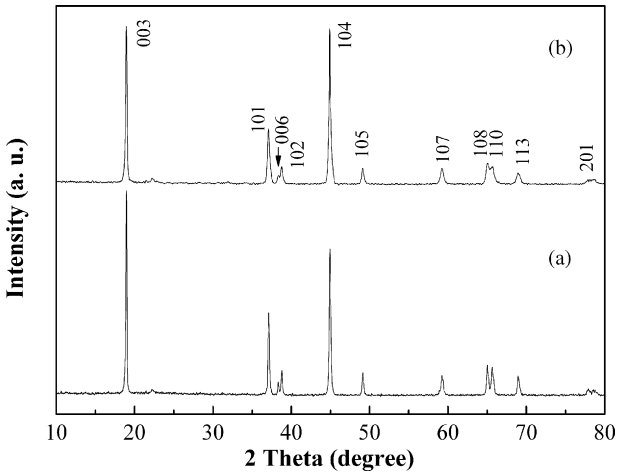

Fig. 7. XRD patterns of $LiNi_{1/3}Co_{1/3}Mn_{1/3}O_2$ after charge–discharge 30 cycles. (a) RP and (b) SP.

with smaller amounts of cation mixing. Therefore, it could be concluded that electrochemical properties of the cathode material depend strongly on the structural integrity and morphology character.

4. Conclusions

Well-ordered layered $LiNi_{1/3}Co_{1/3}Mn_{1/3}O_2$ cathode material is successfully synthesized by a rheological phase method, which results in the remarkable morphology and the excellent microstructure by the SEM observation and the XRD experiment. The electrochemical experiments show the higher initial discharge capacities of 167 mAh g^{-1} (3–4.3 V, 20 mA g^{-1}) and 196 mAh g^{-1} (2.5–4.6 V, 200 mA g^{-1}), as well as good cycling performance with the help of rod-shape particle and higher structural integrity, which are superior to those of the material prepared by solid-state method. Therefore, the rheological phase method has been shown here to be promising technique for preparation of $LiNi_{1/3}Co_{1/3}Mn_{1/3}O_2$ cathode materials. Of course, how to control the quantity and the size of the rod-shape particles, and what relation between the quantity and the size of the rod-shape particle with the electrochemical property are to be probed.

Acknowledgement

We gratefully acknowledge the financial support from the National Nature Science Foundation of China (No. 29833090 and No. 29771025).

References

[1] T. Ohzuku, Y. Makimura, Chem. Lett. 1 (2001) 642.
[2] K.M. Shaju, G.V. Subba Rao, B.V.R. Chowdari, Electrochim. Acta 48 (2002) 145.
[3] T.H. Cho, S.M. Park, M. Yoshio, T. Hirai, Y. Hideshima, J. Power Sources 142 (2005) 306.
[4] J. Reed, G. Ceder, Electrochem. Solid-State Lett. 5 (2002) A145.
[5] B.J. Hwang, Y.W. Tsai, D. Carlier, G. Ceder, Chem. Mater. 15 (2003) 3676.
[6] M.S. Islam, R.A. Davies, J.D. Gale, Chem. Mater. 15 (2003) 4280.
[7] D. Li, T. Muta, L. Zhang, M. Yoshio, H. Noguchi, J. Power Sources 132 (2004) 150.
[8] Z. Wang, Y. Sun, L. Chen, X. Huang, J. Electrochem. Soc. 151 (6) (2004) A914.
[9] M.V. Reddy, G.V. Subba Rao, B.V.R. Chowdari, J. Power Sources 159 (2006) 263.
[10] J.T. Sun, W. Xie, L.J. Yuan, K.L. Zhang, Q.Y. Wang, Mater. Sci. Eng. B 64 (1999) 157.
[11] J. Xiao, H. Zhan, Y.H. Zhou, Mater. Lett. 58 (2004) 1620.
[12] J. Sun, L. Yuan, K. Zhang, Thermochim. Acta 105 (2000) 343.
[13] J. Guo, L.F. Jiao, H.T. Yuan, H.X. Li, M. Zhang, Y.M. Wang, Electrochim. Acta 51 (2006) 3731.
[14] A. Rougier, P. Gravereau, C. Delmas, J. Electrochem. Soc. 143 (4) (1996) 1168.
[15] R. Alcantara, P. Lavela, J.L. Tirado, R. Stoyanova, E. Zhecheva, J. Electrochem. Soc. 145 (1998) 730.
[16] B.J. Hwang, R. Santhanam, C.H. Chen, J. Power Sources 114 (2003) 244.
[17] H. Gabrisch, J.D. Wilcox, M.M. Doeff, Electrochem. Solid State Lett. 9 (2006) A360.
[18] Z. Wang, Y. Sun, L. Chen, X. Huang, J. Electrochem. Soc. 151 (2004) A1914.
[19] X.F. Luo, X.Y. Wang, L. Liao, S. Gamboab, P.J. Sebastian, J. Power Sources 158 (2006) 654.
[20] Y.S. He, Z.F. Ma, X.Zh. Liao, Y. Jiang, J. Power Sources 163 (2007) 1053.
[21] J.M. Paulsen, C.L. Thomas, J.R. Dahn, J. Electrochem. Soc. 147 (2000) 861.
[22] Y.J. Shin, W.J. Choi, Y.S. Hong, S.Y.K.S. Ryu, S.H. Chang, Solid State Ion. 177 (2006) 515.